

# **Controlled Ramp-Down of Decaying Spheromak Plasmas**

G. A. Cone and C. R. Sovinec,  
*University of Wisconsin-Madison*  
*Department of Engineering Physics*

*presented at*

The 45<sup>th</sup> Annual Meeting of the American  
Physical Society Division of Plasma Physics

October 27-31, 2003

Albuquerque, New Mexico

## Abstract

It has been observed in numerical 3D simulations of cylindrical spheromaks that closed flux surfaces form after the applied axial electric field has been crowbarred [1]. Recent numerical investigations of self-similar decaying profiles for a reversed-field pinch (RFP) [2] have shown that improved confinement may be possible with controlled ramp-down of the applied electric fields. In this work we investigate the possibility of similar behavior in the context of a spheromak plasma in a simple cylindrical geometry. The evolution of the plasma profiles of the decaying spheromak is observed for various ramp-down rates of the applied axial electric field.

In addition, the effects of temperature-dependent resistivity and a Braginskii collisional parallel thermal conductivity are addressed in sustained and non-driven decaying simulations. Results show that formation of closed flux surfaces during decay lead to a temporary increase in internal energy which may be prolonged by a re-application of current to the open field lines.

## Objectives

- Examine the profile evolution during decay and assess the magnetic topology quality with surface-of-section plots.
- Investigate plasma confinement properties and magnetic topological quality in context of temperature-dependent resistivity and parallel thermal conductivity.
- Address possibility of improved “confinement” with behavior from  $\eta(T)$  and  $\chi_{\parallel}(T)$  and *rampdown simulations*.

## Simulation Descriptions

### “Can” Geometry

- $H/R = 1.5$
- *Uniform  $B_z$*
- *Applied vertical electric field on outer boundary.*
- *Used in both rampdown & confinement studies.*

### SSPX-like Geometry

- Topologically similar to “can” geometry.  $R=0.5$  m.
  - *External solenoid coils drive bias field.*
  - *Driven by radial electric field at bottom boundary*
- *Used for confinement study.*

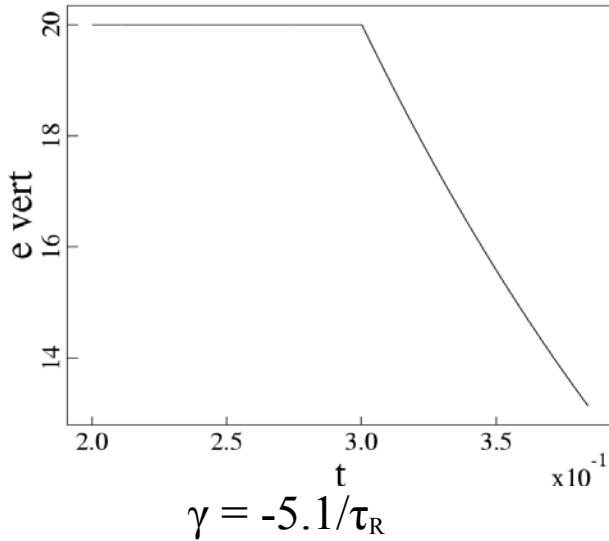
## Ramp-Down Simulations

- Spheromak is driven with a constant electric field up to  $0.3\tau R$  and then the decaying field is applied.
- Simulations performed in “can” geometry with  $R=1.0$  m,  $H=1.5$  m.  $40 \times 60$  biquadratic elements with  $0 \leq n \leq 5$ .
- Conditions before rampdown are:
  - $E = 20$  V/m
  - $S \sim 2,500$

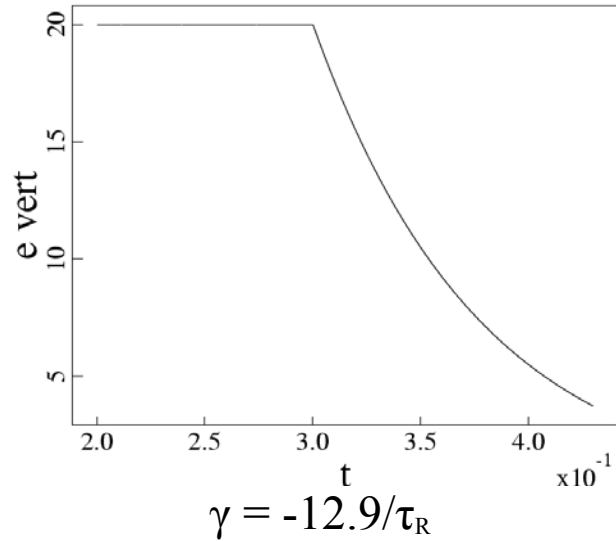
## Ramp-Down Boundary Conditions

Applied vertical electric field exponentially reduced with time from value in the driven phase.

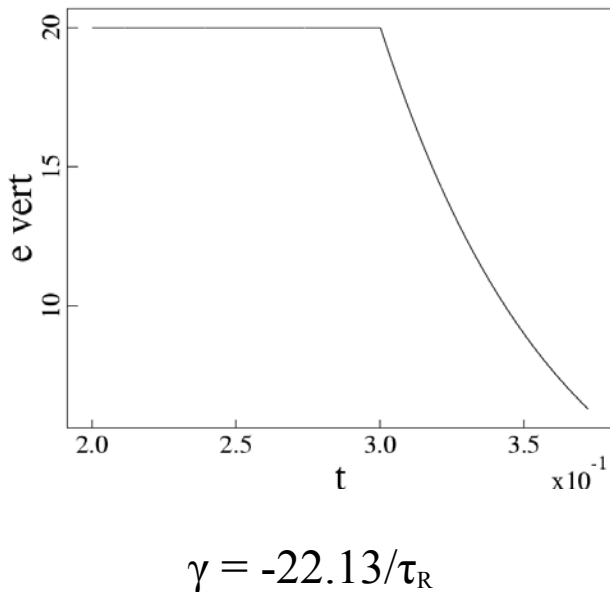
Vert E-field vs. t



Vert E-field vs. t

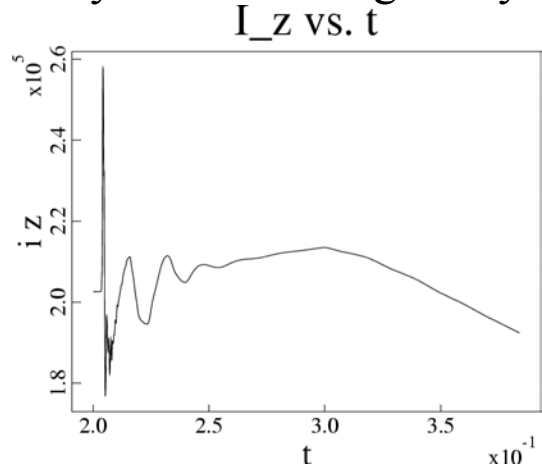
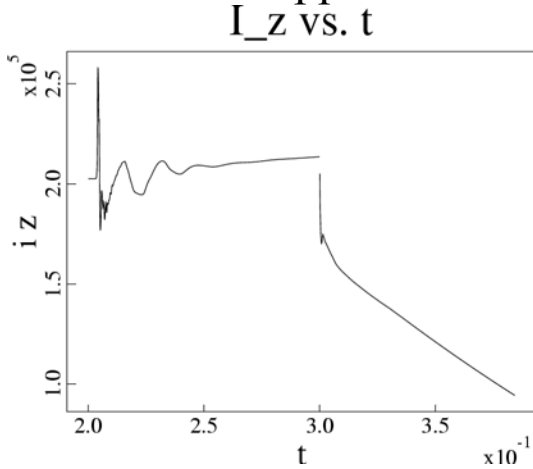


Vert E-field vs. t



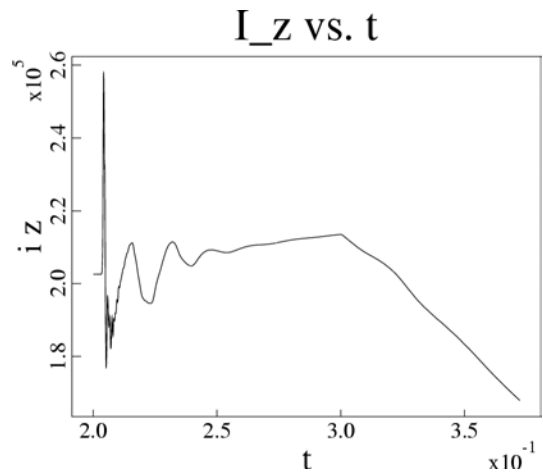
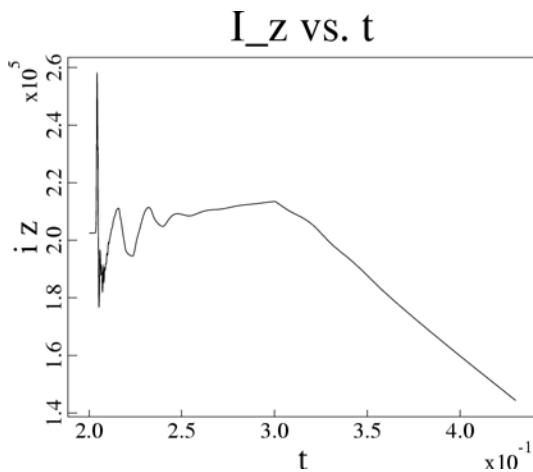
## Ramp-Down Axial Current

Axial current appears to decrease linearly in time during decay.



Crowbarred:  $dI/dt \sim -824 \text{ kA}/\tau_R$

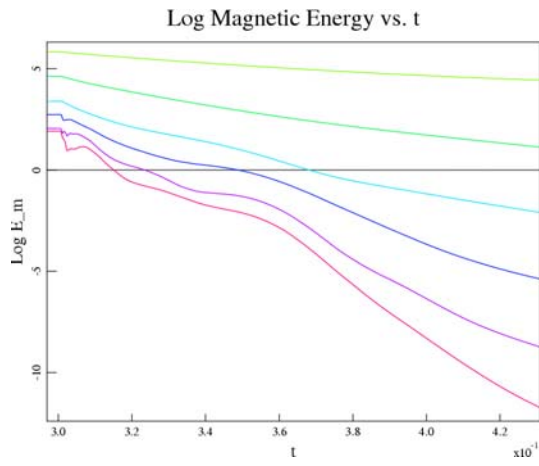
$\gamma = -5.1/\tau_R : dI/dt \sim -278 \text{ kA}/\tau_R$



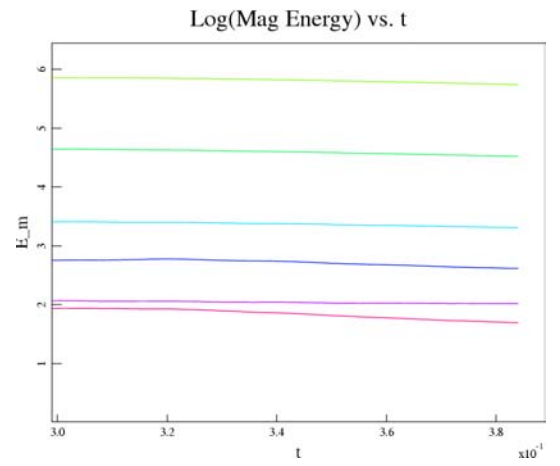
$\gamma = -12.9/\tau_R : dI/dt \sim -560 \text{ kA}/\tau_R$

$\gamma = -22.1/\tau_R : dI/dt \sim -701 \text{ kA}/\tau_R$

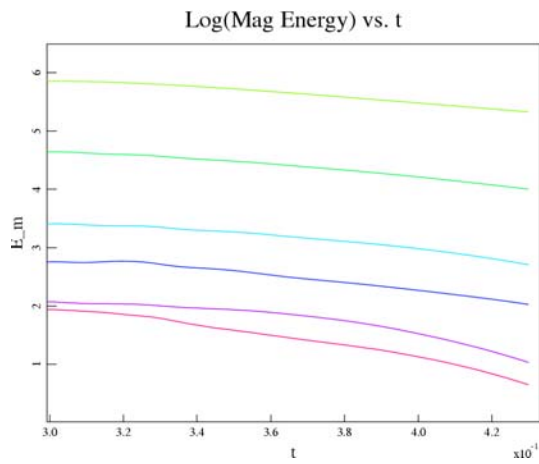
# Evolution of Toroidal Mode Energies



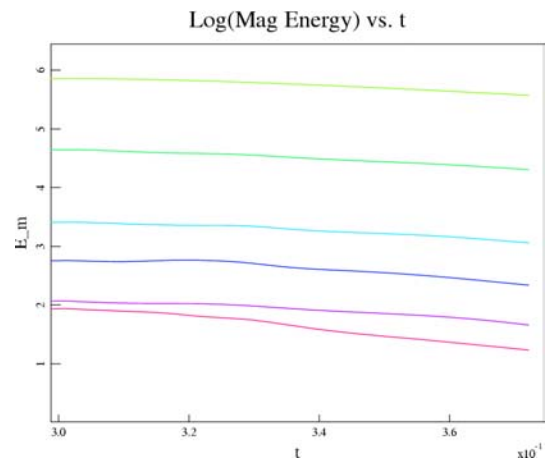
Crowbarred



$$\gamma = -5.1/\tau_R$$



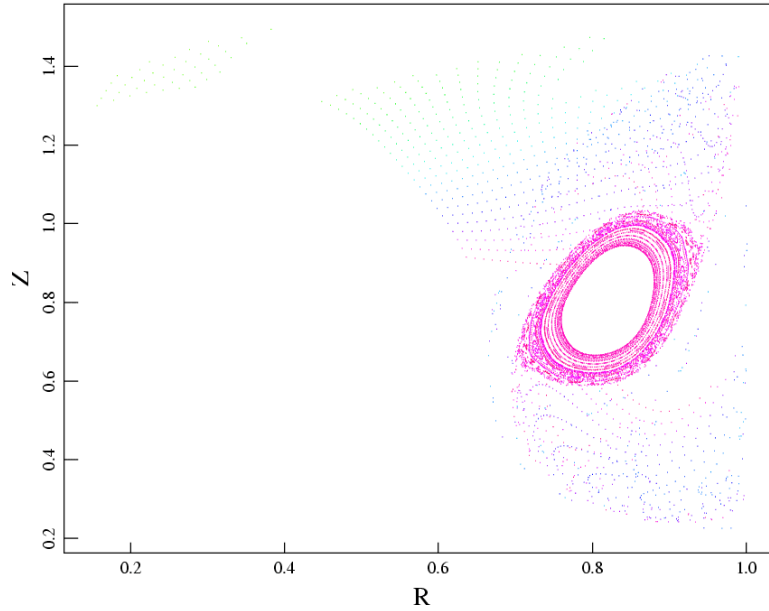
$$\gamma = -12.9/\tau_R$$



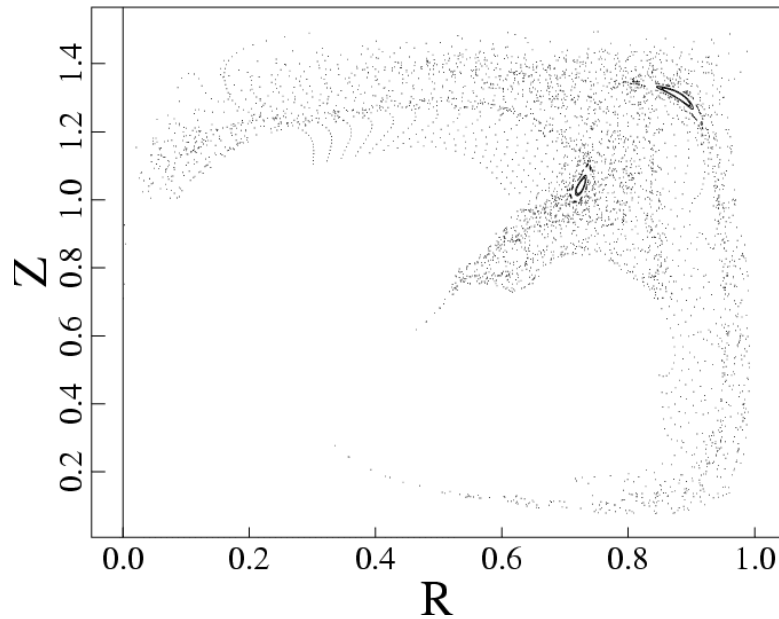
$$\gamma = -22.1/\tau_R$$

# Preliminary Comparison of Closed Flux Surface Generation During Decay

Surface of Section



Crowbarred case show formation of closed flux surfaces around  $t=0.37\tau_R$ .



Ramped down case with  $\gamma=-12.9\tau_R$  forms small helical flux surfaces and shows no growth with time.

## Possible Implications

- Formation of closed flux surfaces demands that magnetic reconnection occurs. The rapid dynamics associated with crowbarring the electrostatic drive and the subsequent decay of magnetic flux on the outer periphery plays a dominant role in the reconnection process.
- Ramping down the electrostatic drive from the sustained state does not induce the dynamics necessary for sufficient reconnection to occur. *More study is needed to explain the mechanisms of this process.*
- The reconnection process is naturally sensitive to the resistivity profile of the plasma. Realistic resistivity profiles are not used for the  $0\text{-}\beta$  simulations. **See following slides on current work being done with temperature dependent resistivity and parallel thermal conductivity for more on this issue!**

## Confinement in Sustained and Decaying Operation

Previous MHD results for spheromaks (Sovinec, *et al.*, PoP **8**, 475, 2001 and Cohen, *et al.*, Nucl. Fusion **43**, 1220, 2003) show significant changes in magnetic topology during the transition from sustainment to decay. Here we use realistic transport models in finite plasma- $\beta$  computations to investigate the impact on confinement.

- Resistivity is temperature-dependent,  $\eta(T) = \eta_0 \left( \frac{T_0}{T} \right)^{3/2}$ .
- Parallel thermal diffusivity is temperature dependent,  
$$\chi(T) = \chi_0 \left( \frac{T}{T_0} \right)^{5/2} .$$
- Heating is Ohmic.
- Walls are cold, and  $T_{wall}$  does not determine the computed core temperatures.

## Validity of Collisional Transport

- Our  $0\text{-}\beta$  MHD results suggest that open-field transport governs confinement during driven conditions.
- Magnetic fields exhibit chaotic scattering (Finn, *et al.*, PRL **85**, 4538, 2002).
  - Although individual magnetic field lines do not fill the volume ergodically, we expect behavior similar to Rechester-Rosenbluth collisional transport if the effective mean-free-path is sufficiently small.
  - We can confirm *a posteriori* that collisionless conditions exist only when and where closed flux surfaces form.

At  $n=5\times 10^{19} \text{ m}^{-3}$  (a value appropriate for SSPX--Stallard, *et al.*, PoP **10**, 2912, 2003) and for  $T=1 \text{ eV}$ ,

- $v_{Te} \cong 6\times 10^5 \text{ m/s}$
- $\tau_e \cong 7\times 10^{-10} \text{ s}$
- $\lambda_e \cong 4\times 10^{-4} \text{ m} \ll L$
- Scaling  $\lambda_e$  with  $T^2$  indicates that  $\lambda_e$  reaches macroscopic scales between 30 and 50 eV.

From this we infer that anisotropic thermal conduction is a good model for sustained (open field) conditions and for the transition to closed flux surfaces during decay.

For high-temperature regions, the collisional parallel diffusion model will be pessimistic without a heat-flux limiter.

## Numerical Benchmark

To verify the recent NIMROD developments for temperature-dependent thermal conductivity we have run a benchmark computation.

- The geometry is a 2D box with a large line-tied guide field.
- Resistivity is uniform.
- Boundary conditions induce a weak uniform parallel current density.
- Perpendicular thermal conductivity is small.

The steady-state electron temperature satisfies

$$-\nabla \cdot \underline{\kappa}(T) \cdot \nabla T = \frac{1}{2}(\gamma - 1)\eta J^2$$

for  $T = T_e = T_i$ , assuming rapid electron-ion temperature equilibration. Temperature within the boundary layers associated with  $\chi_{\perp}$  is then

$$\left(\frac{T}{T_0}\right)^{7/2} = \frac{7\eta J^2(\gamma - 1)}{8T_0 n \chi_0} x(x_{\max} - x) + \left(\frac{T_{\text{wall}}}{T_0}\right)^{7/2},$$

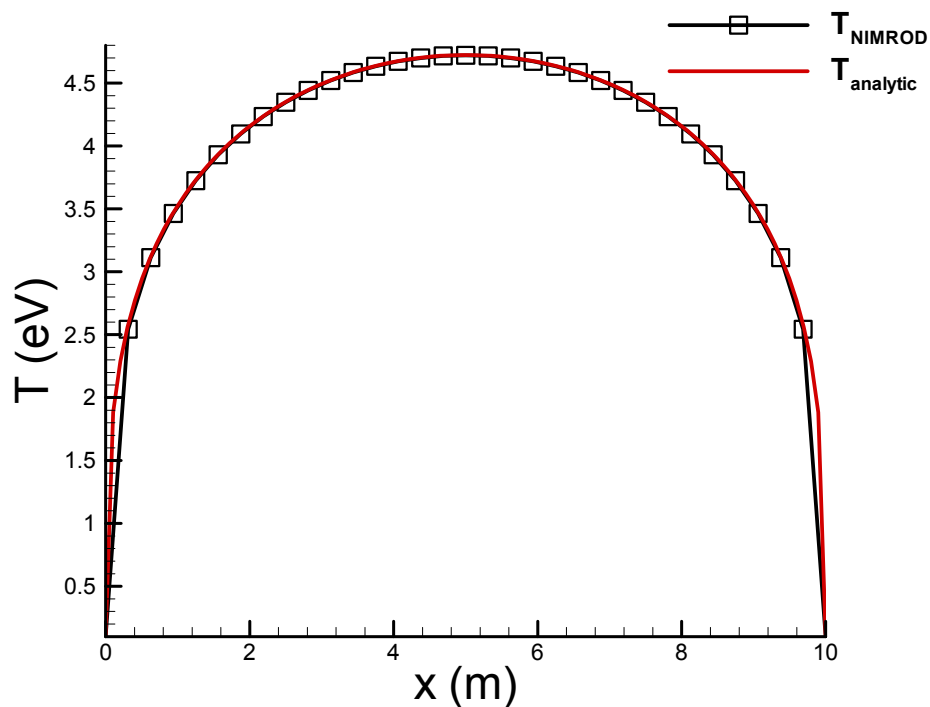
and the peak temperature occurs at  $x_{\max}/2$

$$\left(\frac{T_{\text{peak}}}{T_0}\right)^{7/2} = \frac{7\eta J^2(\gamma - 1)}{32T_0 n \chi_0} x_{\max}^2 + \left(\frac{T_{\text{wall}}}{T_0}\right)^{7/2}.$$

Parameters for the numerical benchmark are:

- $\chi_0=1 \text{ m}^2/\text{s}$  at  $T_0=0.1 \text{ eV}$
- $x_{\text{max}}=10 \text{ m}$
- $\eta/\mu_0=100 \text{ m}^2/\text{s}$
- $n=1\times 10^{19} \text{ m}^{-3}$
- $J=7.96\times 10^3 \text{ A/m}^2$
- Expected  $T_{\text{peak}}=4.72 \text{ eV}$

Results computed with NIMROD using a  $16\times 16$  mesh of biquadratic elements match the expected distribution.

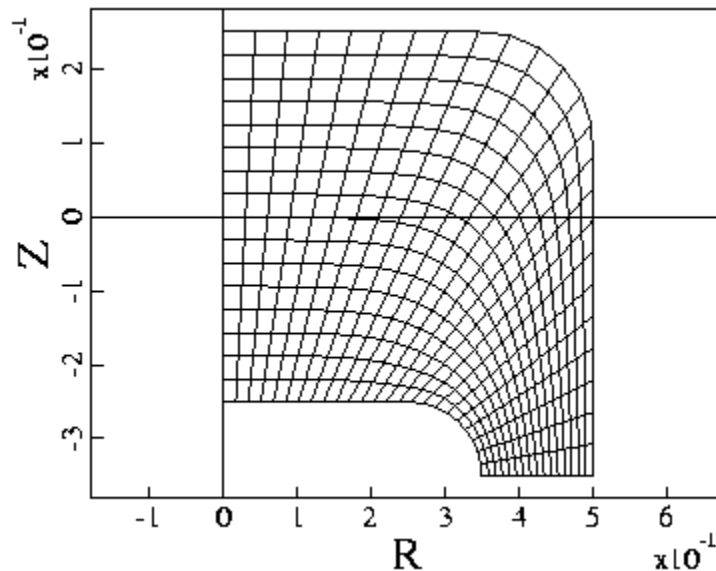


Analytic and numerical temperature profiles for the benchmark calculation.

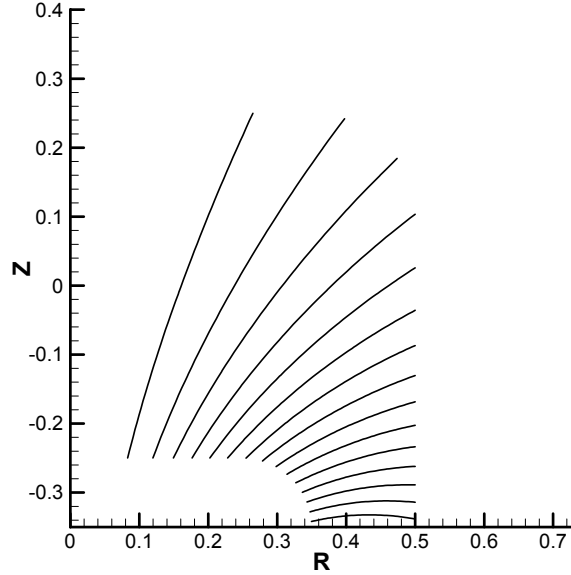
## Finite- $\beta$ Spheromak Simulations

Two geometries:

- 1) Can configuration is similar to that used for basic MHD studies. It has  $R=0.5$  m,  $L_z=0.75$  m.
  - a. Uniform bias field penetrates the top and bottom electrodes.
  - b. Plasma current is by vertical electric field applied along outer surface.
- 2) SSPX-like configuration has a smoothly shaped flux conserver.
  - a. External solenoid coils drive bias field.
  - b. The plasma discharge is driven by electric field across the break between electrodes.



Mesh of bicubic finite elements for SSPX-like configuration.



Vacuum poloidal flux distribution for SSPX-like configuration.

### Other Parameters

#### *Can Simulation*

$$n=3 \times 10^{19} \text{ m}^{-3}$$

$$\frac{\eta(T)}{\mu_0} = 822 \left( \frac{1 \text{ eV}}{T} \right)^{3/2} \text{ m}^2/\text{s}$$

$$\chi_{\parallel}(T) = 400 \left( \frac{T}{1 \text{ eV}} \right)^{5/2} \text{ m}^2/\text{s}$$

$$\chi_{\perp} = 50 \text{ m}^2/\text{s} \sim \chi_{\perp_i}(1 \text{ eV})$$

$$T_{\text{wall}} = 0.1 \text{ eV}$$

$$\nu = 300 \text{ m}^2/\text{s}$$

#### *SSPX Simulation*

$$n=5 \times 10^{19} \text{ m}^{-3}$$

$$\frac{\eta(T)}{\mu_0} = 822 \left( \frac{1 \text{ eV}}{T} \right)^{3/2} \text{ m}^2/\text{s}$$

$$\chi_{\parallel}(T) = 258 \left( \frac{T}{1 \text{ eV}} \right)^{5/2} \text{ m}^2/\text{s}$$

$$\chi_{\perp} = 21 \text{ m}^2/\text{s} \cong \chi_{\perp_i}(1 \text{ eV})$$

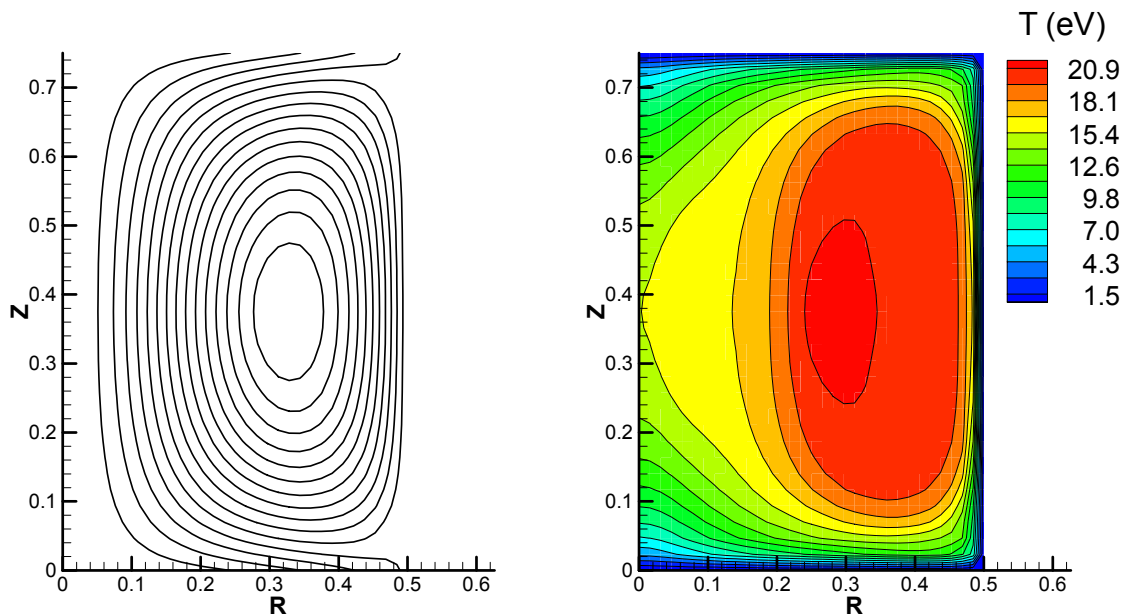
$$T_{\text{wall}} = 0.1 \text{ eV}$$

$$\nu = 100 \text{ m}^2/\text{s} \text{ \& } 300 \text{ m}^2/\text{s}$$

The can configuration produces a broad temperature profile with peak values of 20-30 eV in driven conditions.

## Can Geometry Results

- Cases with constant current drive of  $I_{ext}=187.5$  kA produce maximum temperatures of  $\sim 20$  eV.
  - Scoping study has  $16 \times 16$  biquadratic elements with  $0 \leq n \leq 2$  produces 282% flux amplification,  $T_{max}=22$  eV.

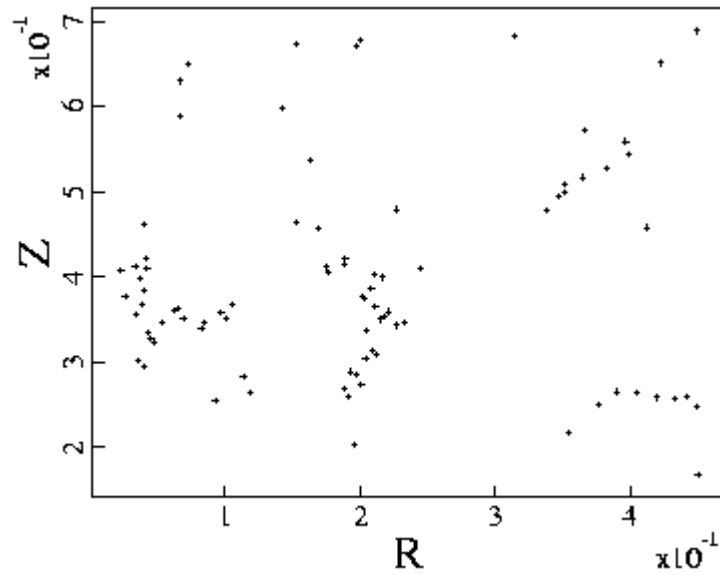


$n=0$  Poloidal Flux

$n=0$  Temperature

- A higher resolution case with a  $32 \times 32$  mesh of biquadratic elements and  $0 \leq n \leq 5$  has so far produced 207% flux amplification and  $T_{max}=19.4$  eV. Magnetic energy has not saturated, however.

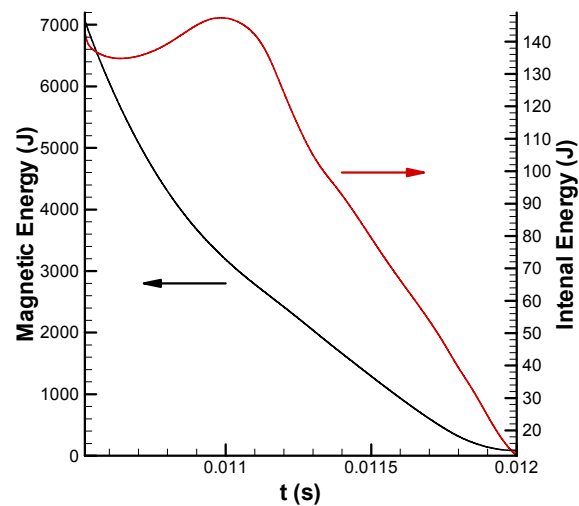
- Temperatures are determined by the open-field topology and parallel thermal transport during sustainment.



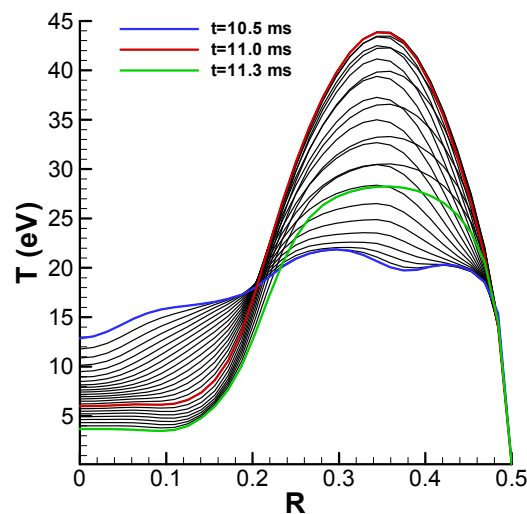
Poincaré surface of section for the driven can configuration.

When the drive is removed, closed flux surfaces form, as in  $0-\beta$  computations, and the temperature profile becomes peaked with a maximum value that initially increases.

- The constant current drive is replaced by a crowbarred circuit at  $t=10.5$  ms.

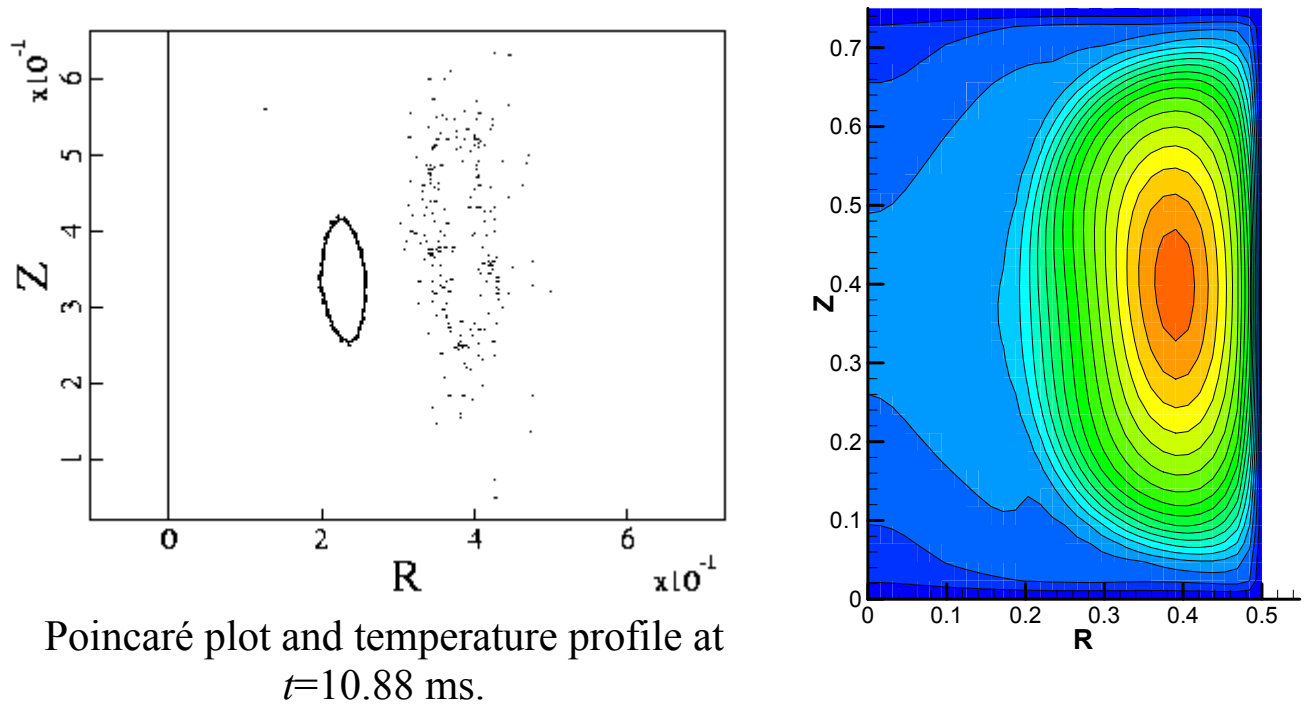
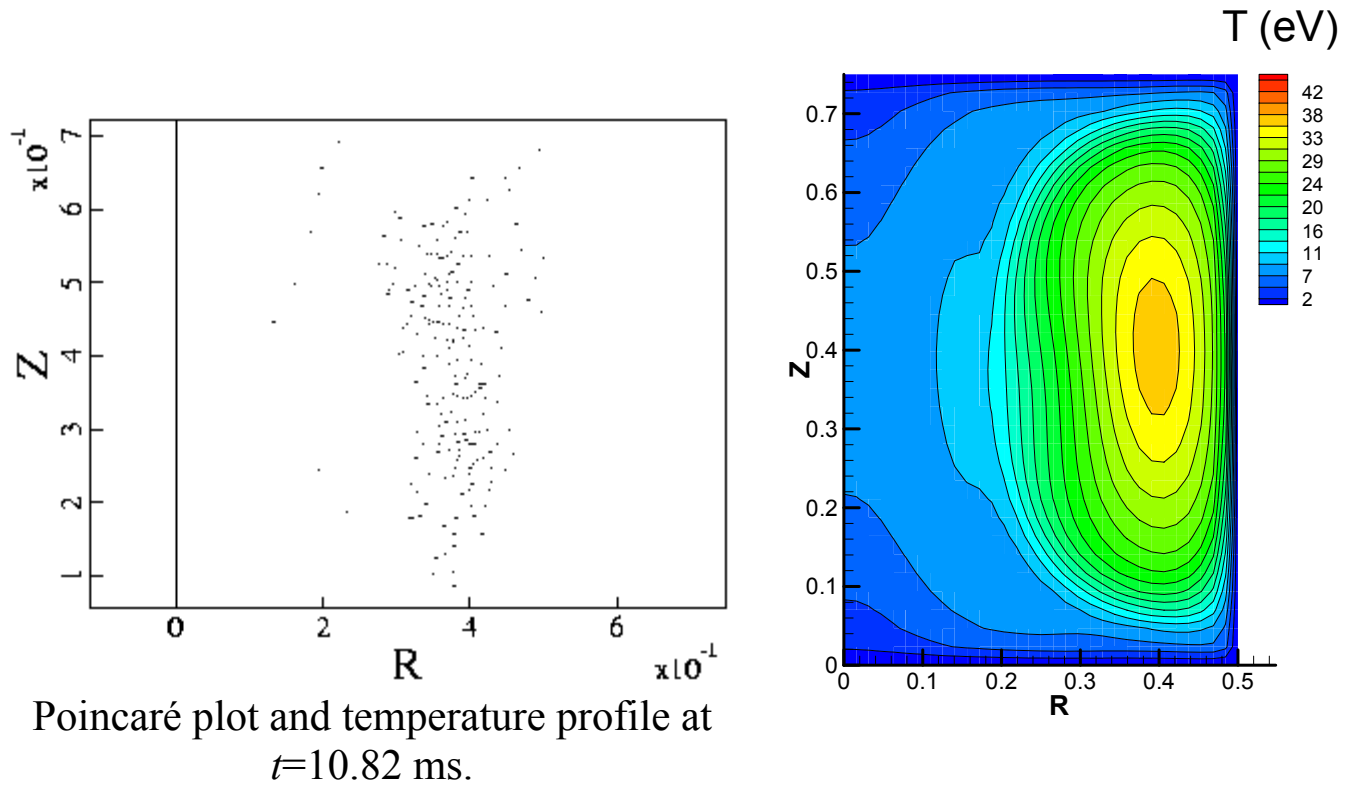


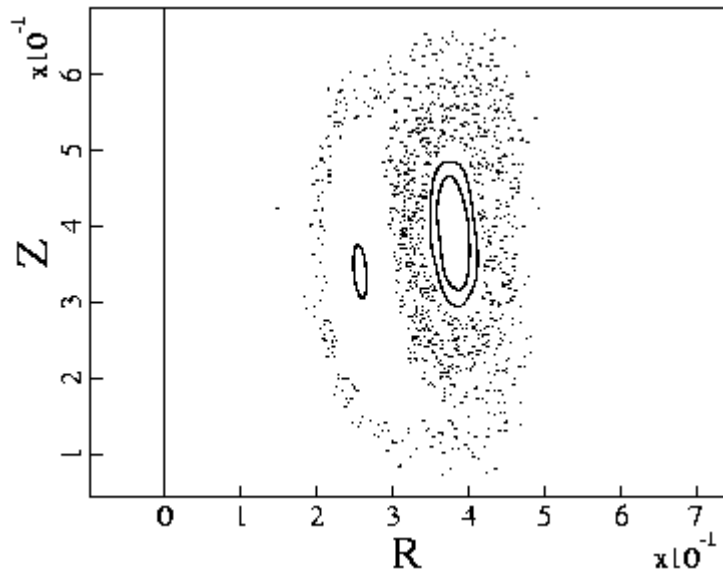
Internal energy increases in time while magnetic energy decays.



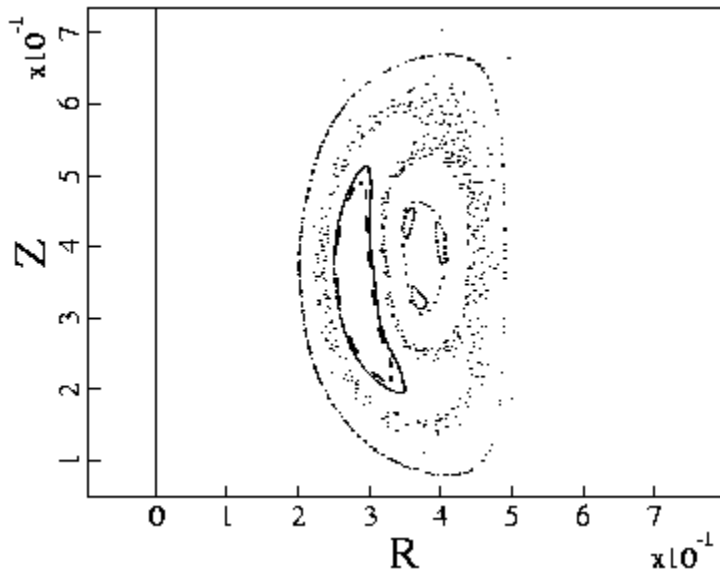
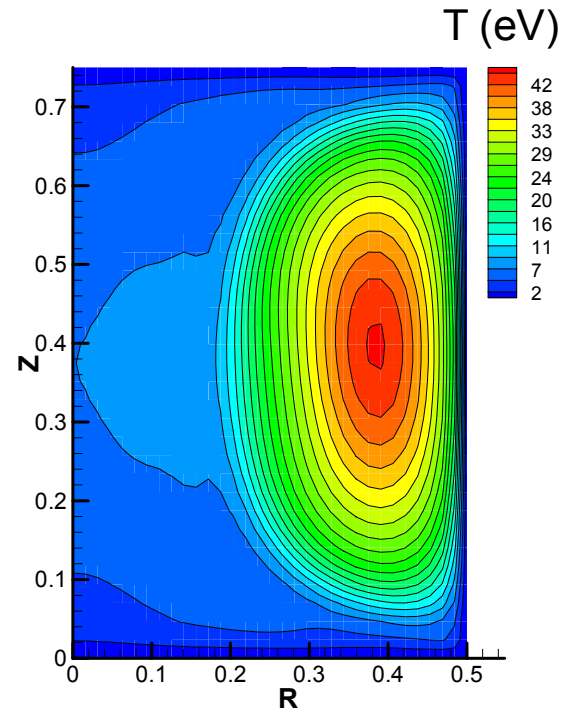
Midplane traces of  $T_{n=0}$  ( $10.5 \leq t \leq 11.3$  ms in steps of 30  $\mu$ s).

Temperature change results from flux surface formation.

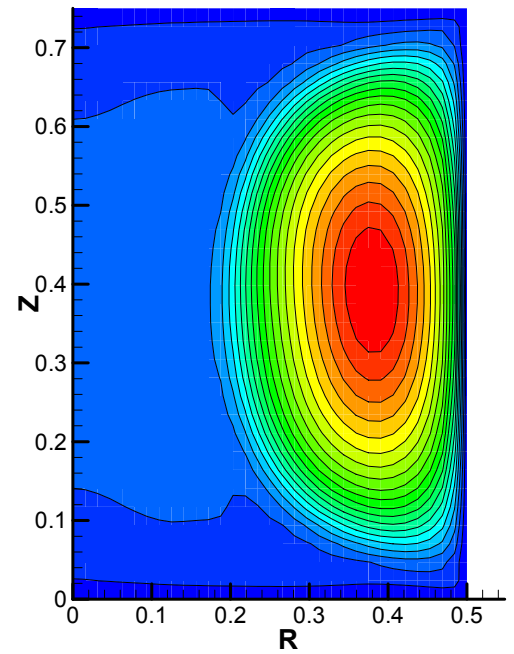




Poincaré plot and temperature profile at  $t=10.94$  ms.

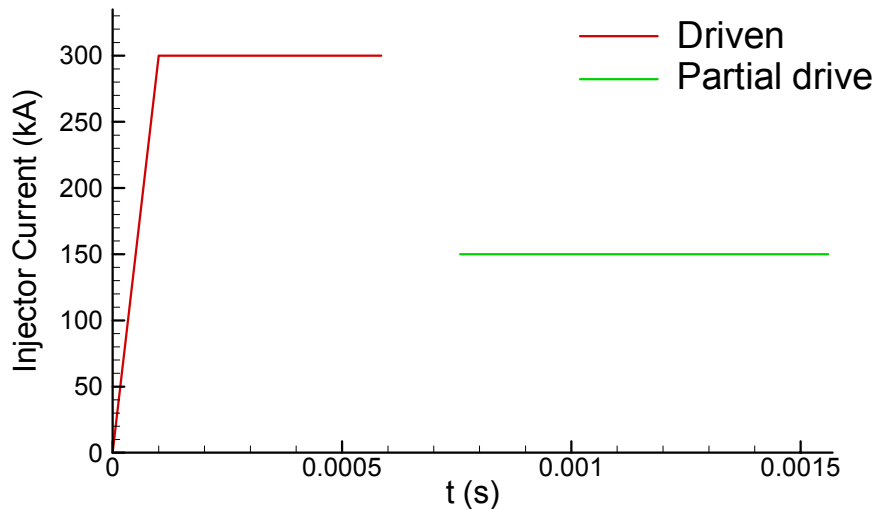


Poincaré plot and temperature profile at  $t=11.03$  ms.

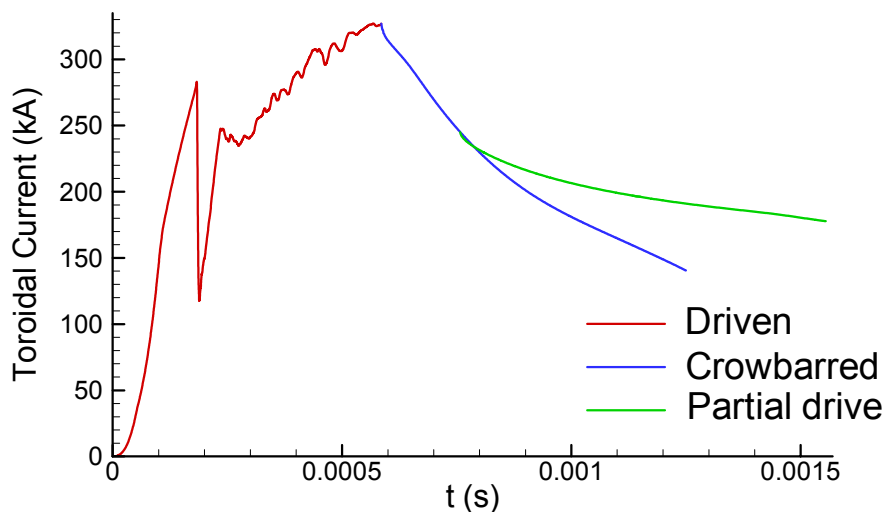


## SSPX Simulation Results

- Three simulations using a  $16 \times 24$  mesh of bicubic elements with  $0 \leq n \leq 2$  address 1) initial drive and sustainment, 2) free decay, and 3) partially driven decay.

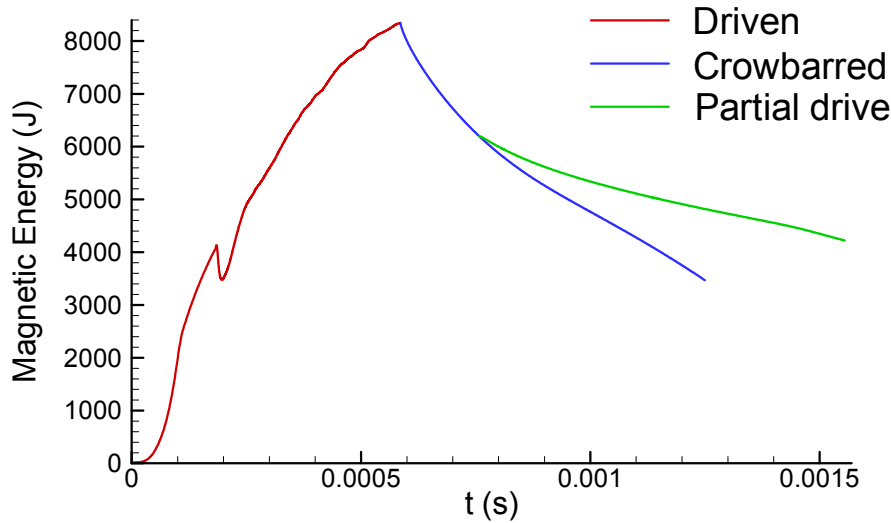


During the initial drive and partial drive stages, the injector current is programmed as shown.

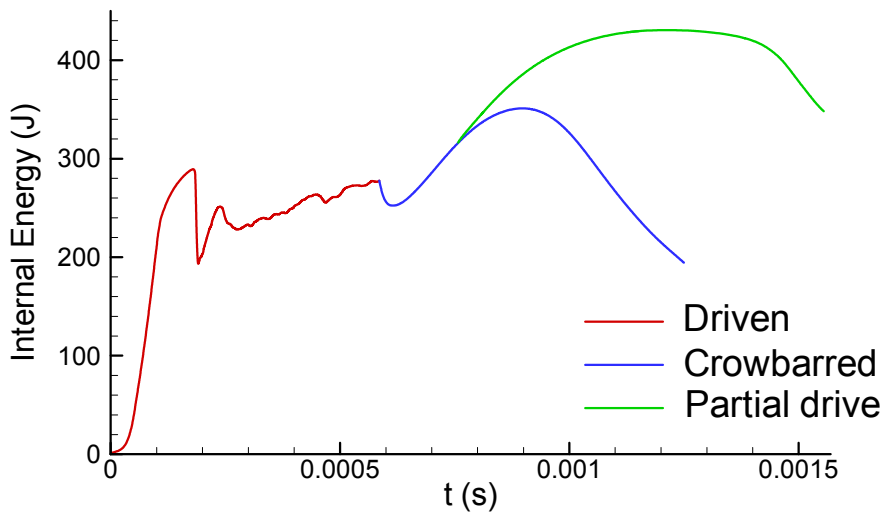


The plasma toroidal current saturates at slightly more than the injected current during drive. Later, partial drive reduces decay.

After the initial drive is removed, energy lost from the magnetic field helps heat the plasma, and internal energy increases.

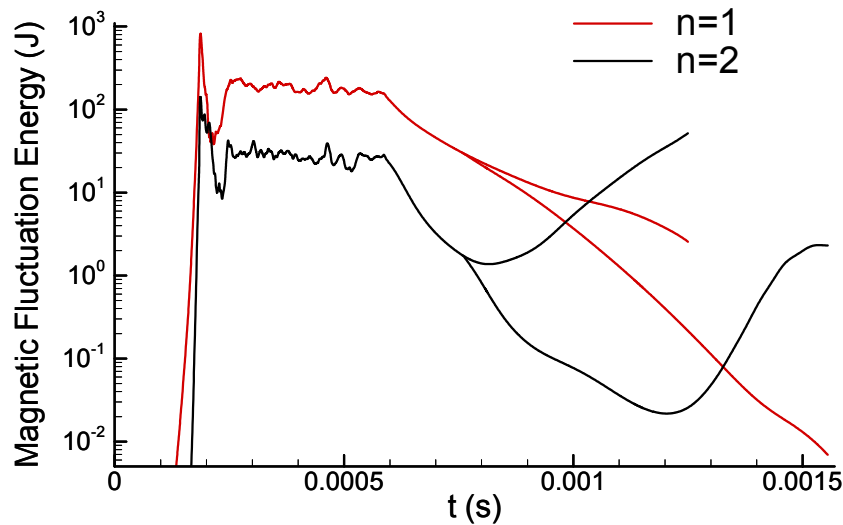


At  $t=1$  ms, magnetic energy loss amounts to 4.9 MW in the crowbarred case, and 2.5 MW in the partially driven case.

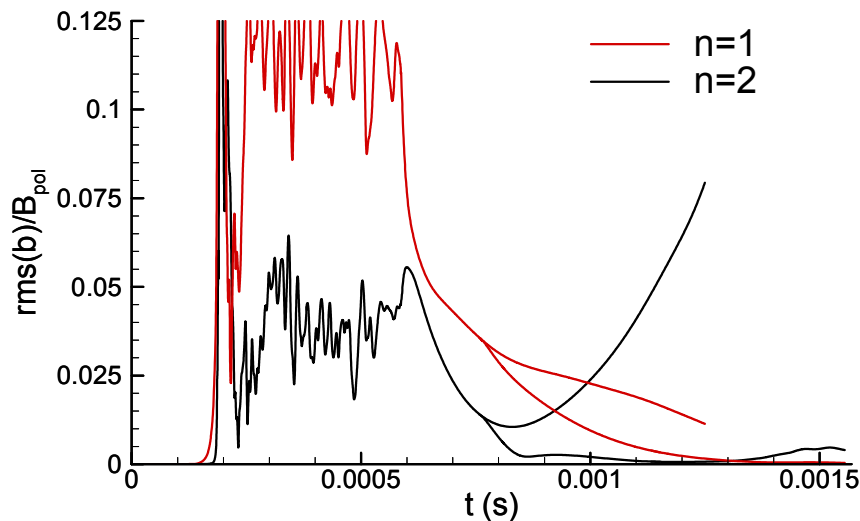


Internal energy is larger and maintained over a longer period of time when partial drive is applied.

Magnetic fluctuations initially decrease when the drive is removed. Eventually, the n=2 mode is excited (similar to Sgro, Mirin, and Marklin, PF 30, 3219, 1987).



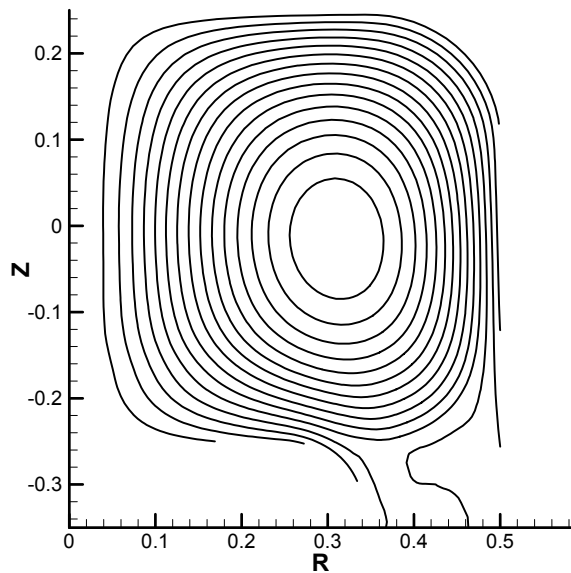
Partial drive enhances fluctuation energy decay and prolongs the onset of the n=2 mode.



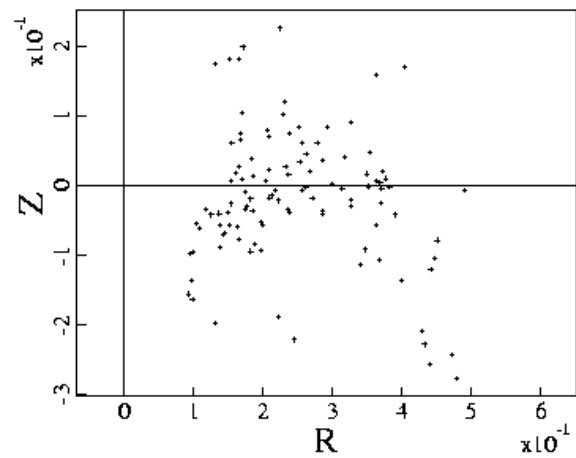
The rms magnetic signals from a probe located at the outboard midplane show fluctuation levels of  $<1\%$  during partial drive.

The improved energy confinement results from flux-surface formation after the drive is removed, as in the can geometry.

### Driven State

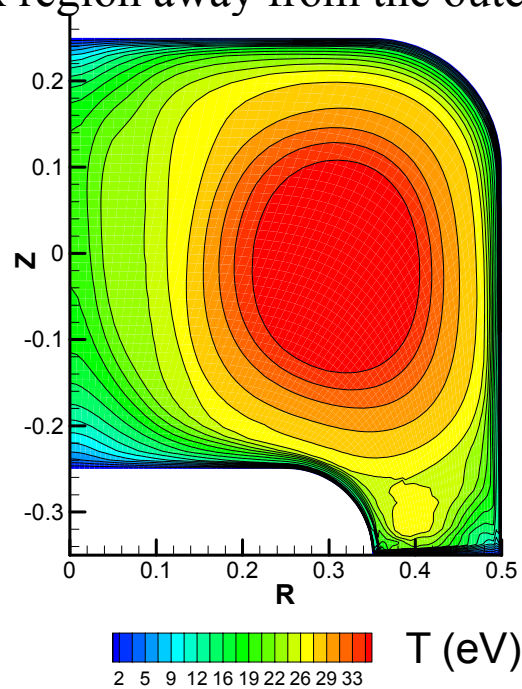


Poloidal flux contours show 305% amplification from  $n=1$  MHD activity at  $t=0.58$  ms.

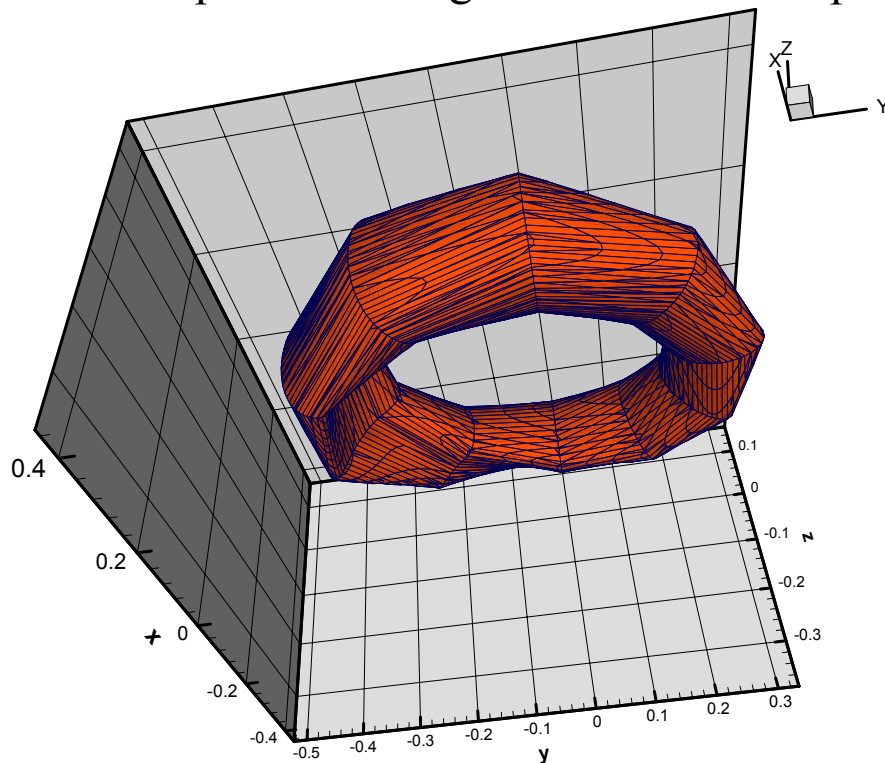


Poincaré plots show that there are no large closed-flux surfaces during full sustainment.

The peak temperature during drive is 37 eV—possibly higher than the can configuration because the stretched bias field keeps the amplified-flux region away from the outer wall.

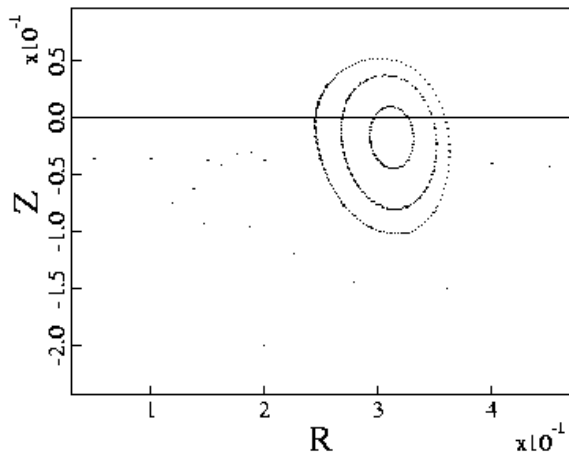


The  $n=0$  component of  $T$  again shows a broad profile.

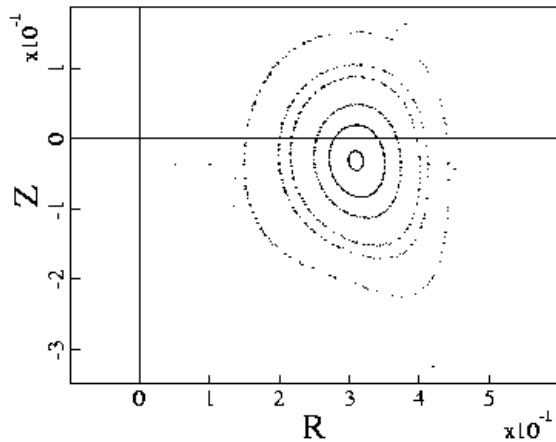
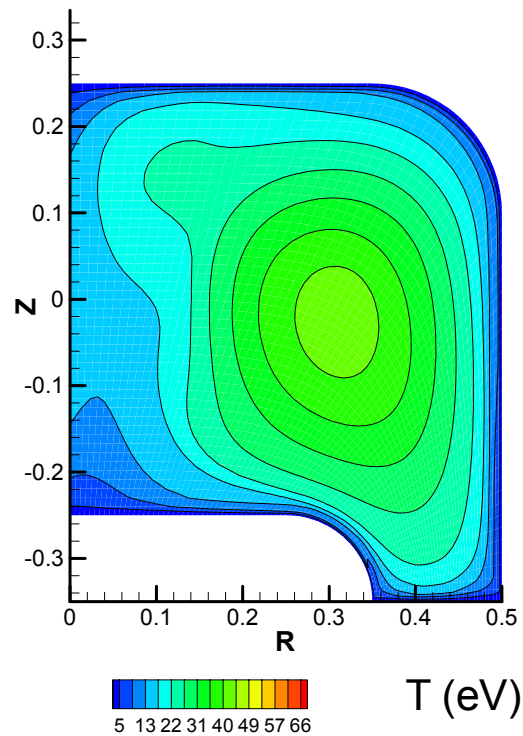


With a 3D view, the  $T=37$  eV isosurf. shows  $n=1$  deformation.

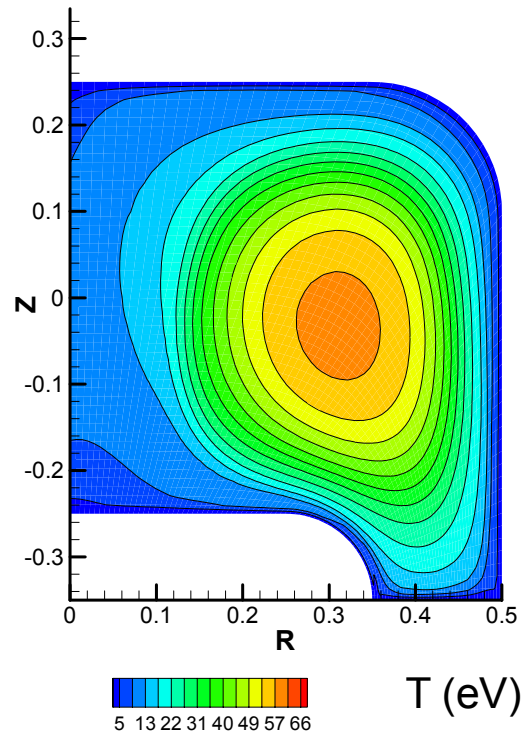
- During the free decay, large closed flux surfaces form, and the peak temperature increases with internal energy.



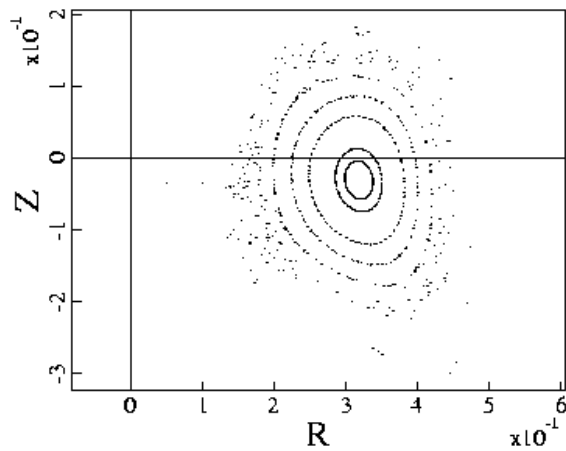
Poincaré plot and temperature profile at  $t=0.63$  ms.



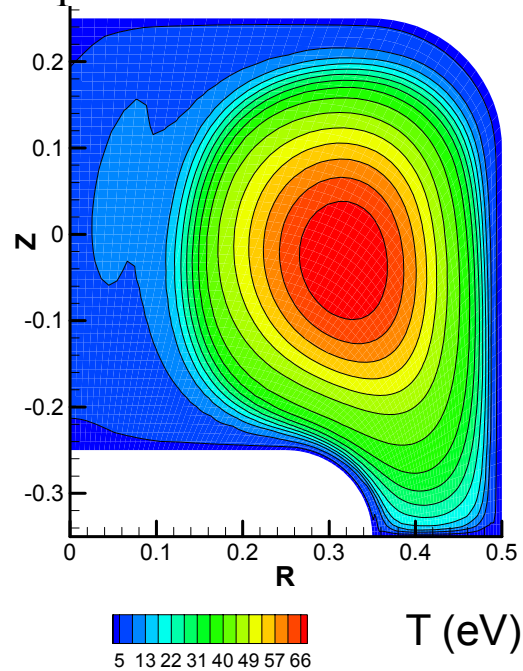
Poincaré plot and temperature profile at  $t=0.76$  ms.



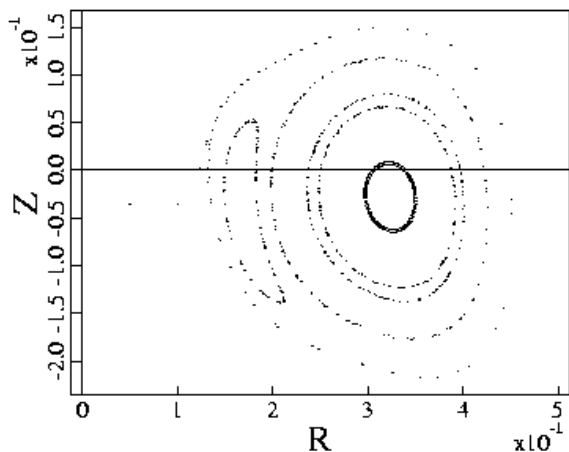
- During the free decay, the peak temperature is 70.4 eV



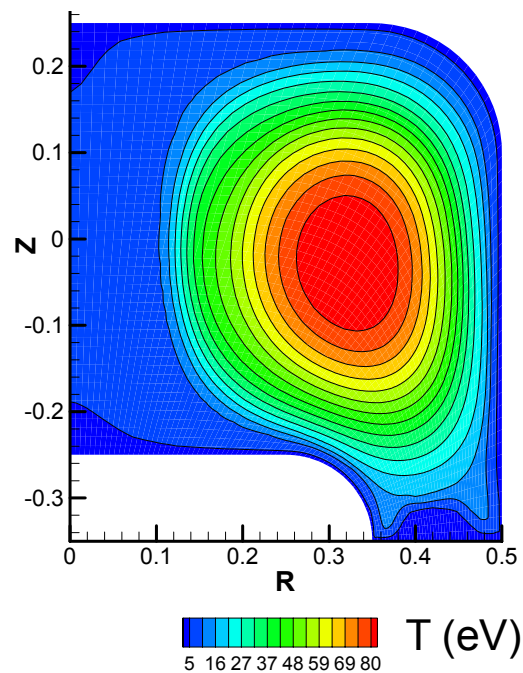
Poincaré plot and temperature profile at  $t=0.91$  ms.



- With partial drive, the fluctuation level is lower, flux surfaces remain larger, and the added toroidal field pressure helps keep plasma off the electrodes. Here,  $T_{peak}=86$  eV.



Poincaré plot and temperature profile at  $t=1.48$  ms.



## Discussion

- The temperature dependence of the parallel thermal conduction is important for providing edge energy confinement during the initial drive.
- Two-dimensional driven computations (not presented) with the same parameters show peak temperatures that are comparable to the driven-spheromak temperatures ( $\sim 35$  eV in the SSPX configuration).
- An interplay of inductive effects and temperature-dependent transport coefficients produces the low-fluctuation, high-confinement states.
  - The  $n=1$  mode of the open-field current channel decays rapidly when the drive is removed—the open-field plasma cools, and pinch current subsides.
  - Low-resistivity plasma within the hot flux surfaces retains toroidal current associated with the  $n=1$ -generated poloidal flux.
  - The influence of the MHD activity on the magnetic topology during drive and decay are consistent with earlier  $0-\beta$  simulation results (Finn, *et al.*, PRL **85**, 4538, 2002 and Sovinec, *et al.*, PoP **8**, 475, 2001).
- The realistic parameters and collisional temperature dependencies make the MHD results quantitatively consistent with SSPX results (McLean, *et al.*, PRL **88**, 125004, 2002).
  - Temperature profiles—peak values within  $\sim 30\%$ .
  - Magnetic fluctuations are  $\sim 1\%$  during partial drive.
  - Magnetic energy decay of  $\sim 2-4$  MW during partial drive.

## Future Work

- Numerical convergence:
  - Retaining  $n > 2$  Fourier components may have some quantitative impact.
  - The poloidal plane is likely well resolved by the bicubic elements (including resolution of anisotropic transport), but this needs to be verified.
- Modeling:
  - Extending the computational domain farther into the gun will allow us to put more of the bias flux there, as in the experiment. This will result in less tension on the flux surfaces towards the electrodes after the drive is removed.
- Physics studies:
  - Investigate proposed differences between free decay and partial drive and their impact on  $n=1$  and  $n=2$  modes.
  - Understand magnetic fluctuation power transfer during the transient.
  - Apply what we learn to optimizing flux-surface formation and avoiding MHD activity that occurs later in time.

## Acknowledgments

We are indebted to Ken Fowler for discussions regarding the applicability of collisional transport coefficients and the importance of their temperature-dependence.

We would also like to thank our *system administrator*, Tony Hammond, for making the simulations reported here possible by keeping our Linux cluster on-line.